Phys. Status Solidi B **248**, No. 7, 1576–1580 (2011) / **DOI** 10.1002/pssb.201001125

physica status solidi b
www.pss-b.com
basic solid state physics

GaAs–MnAs nanowires

Janusz Sadowski[*,1,2], Aloyzas Siusys[2], Andras Kovacs[3], Takeshi Kasama[3], Rafal E. Dunin-Borkowski[3,4], Tomasz Wojciechowski[2], Anna Reszka[2], and Bogdan Kowalski[2]

[1] MAX-Lab, Lund University, P.O. Box 118, 221 00 Lund, Sweden
[2] Institute of Physics, Polish Academy of Sciences, al. Lotników 32/46, 02-668 Warszawa, Poland
[3] Center for Electron Nanoscopy, Technical University of Denmark, Kgs. Lyngby 2800, Denmark
[4] Institute for Microstructure Research, Peter Gruenberg Institute, Forschungszentrum Juelich, 52425 Juelich, Germany

Received 1 October 2010, revised 22 October 2010, accepted 25 October 2010
Published online 27 May 2011

Keywords ferromagnetic semiconductors, molecular beam epitaxy, nanowires

[*] Corresponding author: e-mail janusz.sadowski@maxlab.lu.se, Phone: +46 46 2224310, Fax: +46 462224710

Different strategies for obtaining nanowires (NWs) with ferromagnetic properties using the molecular beam epitaxy (MBE) grown nanostructures combining GaAs and Mn were investigated. Four types of structures have been studied: (i) self-catalyzed GaAs:Mn NWs grown at low temperatures on GaAs(100) substrates; (ii) GaAs:Mn NWs grown at high temperatures on Si(100) substrates; (iii) GaAs–GaMnAs core–shell NW structures; (iv) GaAs–MnAs core–shell NW structures grown on Si(100). Structures of types (i), (iii), and (iv) exhibit ferromagnetic properties.
Right: Scanning electron microscopy image of Mn doped GaAs NWs with Ga droplets at the tops, grown by MBE on oxidized Si(100) substrate in the autocatalytic growth mode.

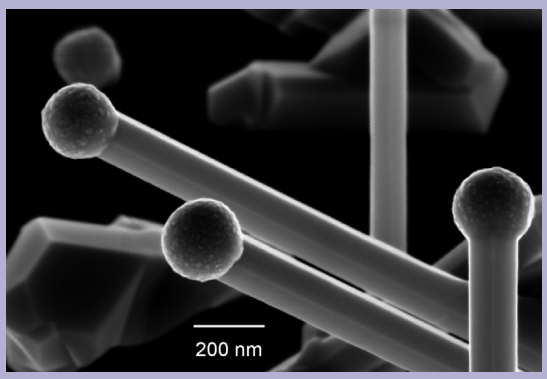

1 Introduction Nanowires (NWs) combining the ferromagnetic semiconductors and/or ferromagnetic metals with semiconducting nanostructures can bring interesting applications for example in nonvolatile memory devices with magnetic information storage [1]. The possibility of obtaining such nanoscale structures by self-assembled growth methods has some advantage in comparison to the methods involving nanolithography techniques, typically used in the semiconductor technology. We have combined the self-assembled GaAs NWs grown by molecular beam epitaxy (MBE) on Si substrates with ferromagnetic materials such as GaMnAs and MnAs. The use of Si substrates with thin native oxide surface layer for the MBE growth of GaAs, at proper conditions leads to the growth of NWs catalyzed by Ga droplets spontaneously formed at the SiO_2/Si surface. The Ga droplets are quite uniform and have diameters in the range of 150–200 nm, which also determines the diameter of GaAs NWs. The GaAs NWs are then used as the templates for deposition of GaMnAs and/or MnAs with use of the same MBE system, additionally equipped with the Mn source.

2 MBE growth methods used for GaAs:Mn NWs formation

2.1 GaMnAs NWs grown at low substrate temperature The MBE growth of GaMnAs ternary alloy – a canonical ferromagnetic semiconductor first obtained in 1996 [2] requires the very low substrate temperatures, in order to overcome the low Mn solubility limit in GaAs [3]. It was shown by several groups that during low temperature MBE growth of GaAs it is possible to obtain a GaMnAs ternary alloy with Mn content up to 10% (even 20% in some special MBE growth conditions) [4–10]. GaMnAs with high enough Mn content (higher than about 1%) exhibit a paramagnetic-to-ferromagnetic phase transition due to the

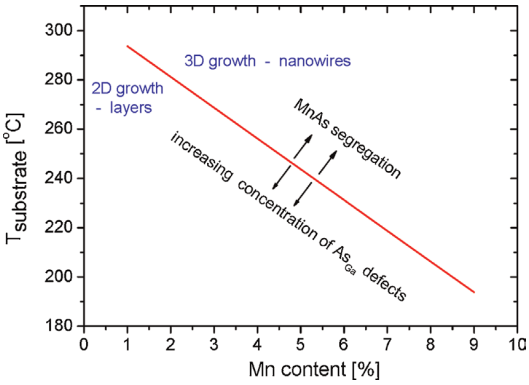

Figure 1 (online color at: www.pss-b.com) Schematic (simplified) temperature diagram for low temperature MBE growth of GaMnAs ternary alloy.

interactions between spins of carriers (holes) and atomic spins of Mn ions ($S = 5/2$) located at Ga sites in the GaAs host lattice [11]. Mn partially substituting Ga is acting as a shallow acceptor, providing high concentrations of holes, essential for occurrence of ferromagnetic phase transition in GaMnAs. On the other hand, if the substrate temperature during the MBE growth of GaMnAs is higher than optimum, the segregation of nanoislands of binary MnAs compound occurs at the GaMnAs surface. The simplified temperature diagram showing the regions of growth of uniform GaMnAs ternary alloy and phase segregated GaMnAs:MnAs system is shown in Fig. 1.

The MBE growth of optimum quality GaMnAs takes place in the vicinity of a phase segregation line, *i.e.*, at the temperature which is lower than the MnAs segregation threshold but high enough to minimize the concentration of As antisite defects occurring during the low temperature MBE growth of GaAs [12]. The As antisites, which are double donors in GaAs, reduce the concentration of holes in GaMnAs and thus decrease the paramagnetic-to-ferromagnetic phase transition temperature [11].

It was noticed by us, and published elsewhere [13] that in the case when the GaMnAs MBE growth is continued in the presence of MnAs segregation then the growth mode changes from two-dimensional layer-by-layer growth to the three-dimensional growth of NW-like structures.

Figure 2 shows the examples of NWs grown in these conditions with Mn/Ga flux ratios equal to 1 and 3%.

As shown in Fig. 2 the NWs obtained via the MBE growth of GaMnAs above the MnAs segregation threshold are very much disordered and highly tapered. This is due to the low growth temperatures (350 °C), much lower than the temperatures typically applied for growth of GaAs NWs (550–650 °C). The densities of NWs are proportional to the Mn/Ga flux ratio, but their parameters like lengths and diameters are difficult to control. It was shown elsewhere [13] that the NWs of this type exhibit ferromagnetic properties.

2.2 Mn doped GaAs NWs grown at high temperature Since the low temperature MBE growth of

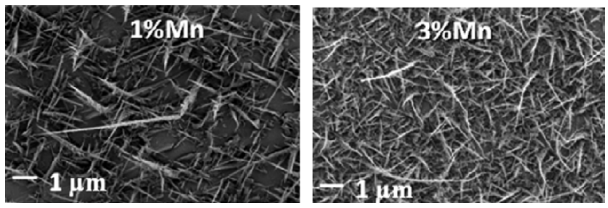

Figure 2 Scanning electron microscopy (SEM) pictures of GaAs:Mn NWs grown on GaAs(100) at the substrate temperature of 350 °C with Mn/Ga flux ratios of 1 and 3%.

NWs described in the previous section does not allow to obtain uniform NWs with well controlled parameters we have used another approach, namely Mn doping during GaAs NWs growth at high substrate temperatures, in the range of 590–630 °C. We have used the NW growth method which does not need any external NW growth catalyst such as most frequently used gold nano-droplets. It was reported by A. Fonctuberta i Moral [14] in 2008 that in the case when GaAs substrate is covered with a thin layer of SiO_2 then the small Ga droplets can be formed on SiO_2 surface and they catalyze the NW growth. If the droplets are contacted with the monocrystalline GaAs substrate through small pinholes in the SiO_2 layer then the resulting NWs are in epitaxial relation to GaAs, *i.e.*, they grow along the <111> directions coming out of the GaAs substrate surface [14]. It was noticed later that the same type of growth is possible with use of Si substrates either oxidized, or without the surface oxide [15]. However, the presence of the oxide can be used to order the NWs laterally, by using the prepatterned SiO_2/Si surfaces.

Figure 3 shows SEM pictures of GaAs NWs grown on the SiO_2/Si(100) surface.

The GaAs NWs shown in Fig. 3 have lengths of about 10 µm and diameters of about 150 nm. They have zinc-blende structure, their growth axes are [111], and they have {110} side facets. The sample shown in Fig. 3 was grown at 600 °C for 3 h, with the Ga flux intensity corresponding to GaAs layer growth ratio of 0.2 µm/h.

The Mn doping of GaAs NWs during high temperature MBE growth on silicon does not affect the NW growth. Figure 4 shows SEM pictures of GaAs NWs grown on Si(100) at 590 °C, doped with Mn at Mn/Ga flux ratio of about 1%.

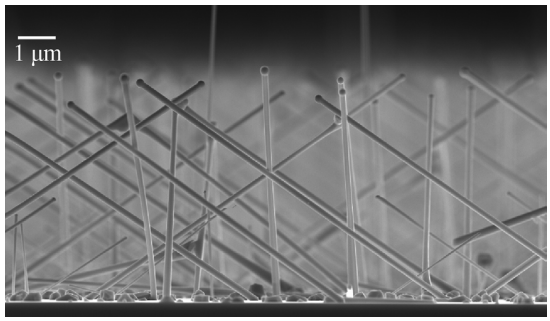

Figure 3 SEM pictures of GaA NWs grown on Si(100) with 5nm thick oxide layer at the substrate temperature of 600 °C.

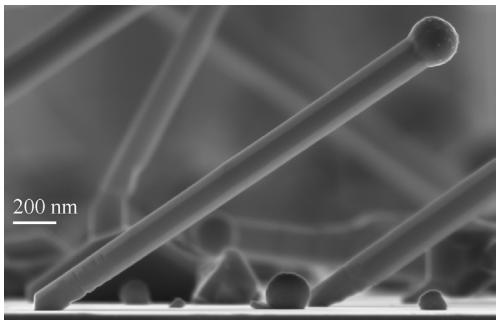

Figure 4 SEM pictures of GaAs:Mn NWs grown on Si(100) at the substrate temperature of 590 °C with the Mn/Ga flux ratio of 1%.

Figure 5 TEM pictures of GaAs:Mn NWs removed from the substrate.

The GaAs:Mn NWs shown in Fig. 4 were also characterized by transmission electron microscope (TEM).

Figure 5 shows that GaAs:Mn NWs have stacking fault defects and their density increases at the top part of NW.

In order to verify if Mn was incorporated into the NWs the line scan energy dispersion X-ray spectroscopy (EDS) measurements were performed along the NW axis. The results are shown in Fig. 6. The EDS scan was performed along the line on a NW shown in the inset.

Figure 6 shows that Mn is accumulated inside the Ga droplet, and in the NW body the Mn content is below the detection limit of the EDS method. However, other measurements performed on the same type of GaAs:Mn NWs such as photoluminescence and transport (not shown here) demonstrate that the NW body is Mn doped to the level of 10^{18} cm^{-3}.

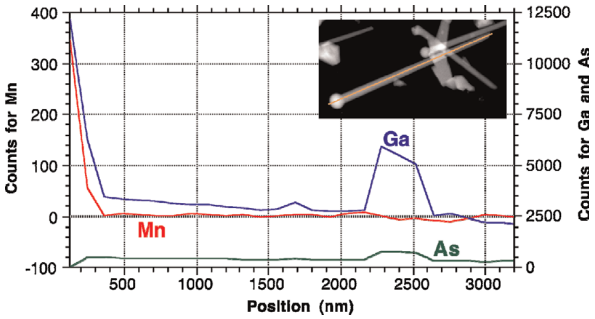

Figure 6 (online color at: www.pss-b.com) EDS line scan showing As, Ga and Mn signal from the individual GaAs:Mn NW shown in the inset. The scan starts at the Ga droplet at the top of the NW.

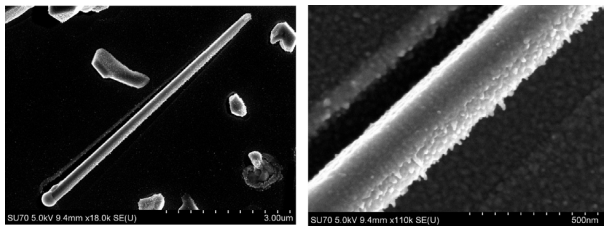

Figure 7 SEM pictures of GaAs–GaMnAs core–shell NWs grown on Si(100).

2.3 GaAs–GaMnAs core–shell NW structures

Since both low temperature growth of GaMnAs NWs and Mn doping of GaAs NWs during high temperature MBE growth did not give satisfactory results (disordered NWs in the former case, and accumulation of Mn inside the catalyzing Ga droplet in the latter) we have tried to grow core–shell structures with GaAs cores grown at high temperature and GaMnAs shells grown at low temperature. This seems to be the only way to combine GaMnAs ferromagnetic semiconductor with NW geometries.

Figure 7 shows an example of this kind of a core–shell structure, with GaAs core NWs grown at 600 °C on oxidized Si(100) and GaMnAs shell with 6% Mn grown at 240 °C.

Figure 7 shows that low temperature grown GaMnAs shells are not perfectly smooth; some island-like structures can be seen on the right panel picture. These are most probably segregated MnAs nano-islands which might originate from slightly too high substrate temperature during growth of GaMnAs shell. This was further confirmed by the results of magnetization measurements shown in Fig. 8.

The high field of saturation magnetization (1000 Oe) as well as high temperature at which the sample shows ferromagnetic properties indicates that magnetic response of the GaAs–GaMnAs core–shell structures is dominated by MnAs, which is probably segregated at the surface of GaMnAs shell. Successful realization of GaAs–GaMnAs core–shell NWs was also recently reported by Rudolph et al. [16], in the case of gold catalyzed NWs grown on GaAs(111)B.

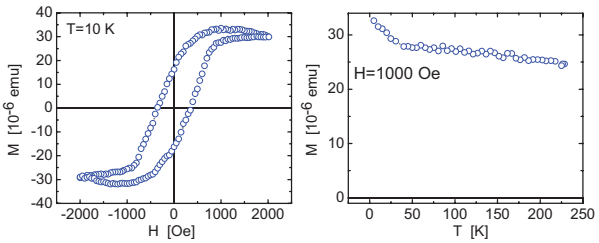

Figure 8 (online color at: www.pss-b.com) Magnetization $M(H)$ and $M(T)$ dependencies measured by SQUID magnetometer for GaAs–GaMnAs core–shell NWs.

2.4 GaAs–MnAs core–shell NW structures

Another possibility for obtaining ferromagnetic NWs based on GaAs and Mn are core–shell structures with semiconducting GaAs cores and ferromagnetic MnAs shells. MnAs is a ferromagnetic metal with NiAs type hexagonal structure. In spite of large difference between zinc-blende GaAs and hexagonal MnAs crystal structures MnAs can be epitaxially grown on GaAs [17]. Most often MnAs layers are grown on GaAs(100) and GaAs(111)B substrate surfaces [18, 19]; however, a successful MBE growth of MnAs on GaAs(110) surface was also reported [20]. Similar to the case of MnAs layers on GaAs(100) surface [21] in MnAs/GaAs(110) system the periodical structure in MnAs epilayers consisting of stripes of ferromagnetic, hexagonal MnAs (α MnAs) and paramagnetic, orthorhombic MnAs (β MnAs) has been observed [20]. The period of the stripe structure was also observed to be MnAs thickness dependent and changing from 200 to 1000 nm in the MnAs thickness range of 50–1000 nm. In the case of Ga catalyzed GaAs NWs investigated here the widths of {110} side facets are in the range of 50–100 nm, which means that the striped structure of MnAs grown on these side facets is unlikely.

Figure 9 shows the GaAs–MnAs core–shell NW structures with the thickness of deposited MnAs of about 5 nm.

Since MnAs shell is grown at low substrate temperature of about 250 °C, it also deposits at the SiO_2/Si surface between the core GaAs NWs. MnAs at the substrate deposits in form of islands, but MnAs deposited at a {110} side facet of GaAs NW looks rather like a continuous layer.

The magnetic properties of the sample with GaAs–MnAs core–shell NW structure (with slightly thinner, 3 nm MnAs shell) are shown in Fig. 10.

Magnetic properties of MnAs–GaAs core–shell NWs are rather typical for MnAs, however since the magnetic moment measured by SQUID was collected from a large piece of sample containing both NWs with different orientations (four different ⟨111⟩ directions are pointing out of the Si(100) substrate, the core GaAs NWs grow in all these directions) and substrate with MnAs nanoislands deposited between the NWs, we cannot determine the magnetic properties of MnAs shell deposited on individual NW. This requires micromagnetic measurements of individual NWs separated from the Si substrate and is a subject of the ongoing projects.

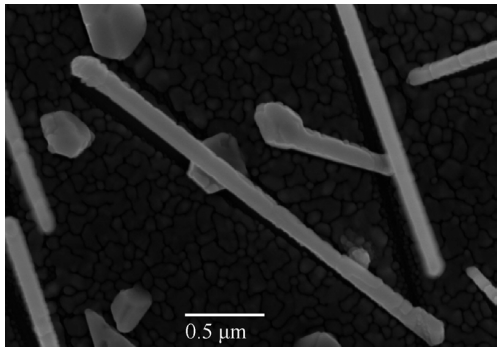

Figure 9 SEM picture of GaAs–MnAs core–shell NWs grown on Si(100) substrates.

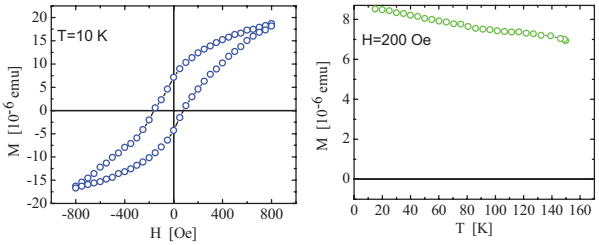

Figure 10 (online color at: www.pss-b.com) $M(H)$ and $M(T)$ dependencies measured by SQUID magnetometer for GaAs–MnAs core–shell NW structure with 3 nm thick MnAs shells.

3 Conclusions We have shown four different examples of nanostructures consisting of GaAs:Mn. GaAs–GaMnAs and GaAs–MnAs NWs which have been grown by MBE without an external catalyst. Highly disordered, short and tapered GaAs:Mn NWs can be obtained by the MBE growth of GaMnAs above the MnAs segregation threshold; GaAs NWs can be lightly doped with Mn during the high temperature MBE growth, finally GaAs–GaMnAs and GaAs–MnAs core–shell NW structures can be grown. The Mn doping efficiency at high temperature GaAs NW MBE growth is limited due to the Mn accumulation inside the catalyzing Ga droplet. The most promising structures which integrate GaAs NWs with magnetic materials based on MnAs and GaMnAs are the core–shell structures with GaAs core NWs grown at high temperatures (600 °C) and GaMnAs or MnAs shells grown at low temperatures (below 300 °C).

Acknowledgements This work has been supported by the EC Network SemiSpinNet (PITN-GA-2008-215368) and by the FunDMS Advanced Grant of the ERC. The authors thank M. Sawicki and O. Proselkov from IP PASc, Warsaw, Poland for SQUID measurements of GaAs–GaMnAs core–shell NWs.

References

[1] S. S. P. Parkin, Science **320**, 190 (2008).
[2] H. Ohno, A. Shen, F. Matsukura, A. Oiwa, A. Endo, S. Katsumoto, and Y. Iye, Appl. Phys. Lett. **69**, 363 (1996).
[3] H. Ohno, Science **281**, 951 (1998).
[4] T. Hayashi, M. Tanaka, T. Nishinaga, and H. Shimada, J. Appl. Phys. **81**, 4865 (1997).
[5] A. Van Esch, L. Van Bockstal, J. De Boeck, G. Verbanck, A. S. van Steenbergen, P. J. Wellmann, B. Grietens, R. Bogaerts, F. Herlach, and G. Borghs, Phys. Rev. B **56**, 13103 (1997).
[6] J. Sadowski, R. Mathieu, P. Svedlindh, J. Z. Domagala, J. Bąk-Misiuk, K. Swiątek, M. Karlsteen, J. Kanski, L. Ilver, H. Åsklund, and U. Södervall, Appl. Phys. Lett. **78**, 3271 (2001).

[7] R. Moriya and H. Munekata, J. Appl. Phys. **93**, 4603 (2003).
[8] K. M. Yu, W. Walukiewicz, T. Wojtowicz, W. L. Lim, X. Liu, Y. Sasaki, M. Dobrowolska, and J. K. Furdyna, Appl. Phys. Lett. **81**, 844 (2002).
[9] K. W. Edmonds, K. Y. Wang, R. P. Campion, A. C. Neumann, C. T. Foxon, B. L. Gallagher, and P. C. Main, Appl. Phys. Lett. **81**, 3010 (2002).
[10] D. Chiba, Y. Nishitani, F. Matsukura, and H. Ohno, Appl. Phys. Lett. **90**, 122503 (2007).
[11] T. Dietl, H. Ohno, F. Matsukura, J. Cibert, and D. Ferrand, Science **287**, 1019 (2000).
[12] A. Wolos, M. Kaminska, M. Palczewska, A. Twardowski, X. Liu, T. Wojtowicz, and J. K. Furdyna, J. Appl. Phys. **96**, 530 (2004).
[13] J. Sadowski, P. Dłużewski, S. Kret, E. Janik, E. Łusakowska, J. Kanski, A. Presz, F. Terki, S. Charar, and D. Tang, Nano Lett. **7**, 2724 (2007).
[14] A. Fontcuberta i Morral, C. Colombo, G. Abstreiter, J. Arbiol, and J. R. Morante, Appl. Phys. Lett. **92**, 063112 (2008).
[15] F. Jabeen, V. Grillo, S. Rubini, and F. Martelli, Nanotechnology **19**, 275711 (2008).
[16] A. Rudolph, M. Soda, M. Kiessling, T. Wojtowicz, D. Schuh, W. Wegscheider, J. Zweck, C. Back, and E. Reiger, Nano Lett. **9**, 3860 (2009).
[17] M. Tanaka, J. P. Harbison, M. C. Park, Y. S. Park, T. Shin, and G. M. Rothberg, Appl. Phys. Lett. **65**, 1964 (1994).
[18] M. Kästner, F. Schippan, P. Schützendübe, L. Däweritz, and K. Ploog, J. Vac. Sci. Technol. B **18**, 2052 (2000).
[19] S. Sugahara and M. Tanaka, J. Appl. Phys. **89**, 6677 (2001).
[20] D. Kolovos-Vellianitis, C. Herrmann, L. Däweritz, and K. H. Ploog, Appl. Phys. Lett. **87**, 092505 (2005).
[21] T. Plake, M. Ramsteiner, V. M. Kaganer, B. Jenichen, M. Kästner, L. Däweritz, and K. H. Ploog, Appl. Phys. Lett. **80**, 2523 (2002).

